International Journal of Astrobiology 13 (2): 112–123 (2014)
doi:10.1017/S1473550413000335

Degradation of microbial fluorescence biosignatures by solar ultraviolet radiation on Mars

Lewis R. Dartnell[1,2,3] and Manish R. Patel[4]

[1]*UCL Institute for Origins, University College London, UK*
[2]*The Centre for Planetary Sciences at UCL/Birkbeck, Earth Sciences, University College London, London, UK*
[3]*Department of Physics and Astronomy, Space Research Centre, University of Leicester, UK*
e-mail: lewis.dartnell@leic.ac.uk
[4]*Department of Physical Sciences, The Open University, Milton Keynes, UK*

Abstract: Recent and proposed robotic missions to Mars are equipped with implements to expose or excavate fresh material from beneath the immediate surface. Once brought into the open, any organic molecules or potential biosignatures of present or past life will be exposed to the unfiltered solar ultraviolet (UV) radiation and face photolytic degradation over short time courses. The key question, then, is what is the window of opportunity for detection of recently exposed samples during robotic operations? Detection of autofluorescence has been proposed as a simple method for surveying or triaging samples for organic molecules. Using a Mars simulation chamber we conduct UV exposures on thin frozen layers of two model microorganisms, the radiation-resistant polyextremophile *Deinococcus radiodurans* and the cyanobacterium *Synechocystis* sp. PCC 6803. Excitation–emission matrices (EEMs) are generated of the full fluorescence response to quantify the change in signal of different cellular fluorophores over Martian equivalent time. Fluorescence of Deinococcus cells, protected by a high concentration of carotenoid pigments, was found to be relatively stable over 32 h of Martian UV irradiation, with around 90% of the initial signal remaining. By comparison, fluorescence from protein-bound tryptophan in *Synechocystis* is much more sensitive to UV photodegradation, declining to 50% after 64 h exposure. The signal most readily degraded by UV irradiation is fluorescence of the photosynthetic pigments – diminished to only 35% after 64 h. This sensitivity may be expected as the biological function of chlorophyll and phycocyanin is to optimize the harvesting of light energy and so they are readily photobleached. A significant increase in a $\sim$450 nm emission feature is interpreted as accumulation of fluorescent cellular degradation products from photolysis. Accounting for diurnal variation in Martian sunlight, this study calculates that frozen cellular biosignatures would remain detectable by fluorescence for at least several sols; offering a sufficient window for robotic exploration operations.

Received 24 June 2013, accepted 30 August 2013, first published online 25 October 2013

Key words: biosignatures, extremophile, fluorescence, life detection, Mars, spectroscopy, ultraviolet radiation.

Introduction

Mars may have provided in its early history an environment conducive for an independent origin of life, but the surface conditions today are no longer hospitable. Low atmospheric pressure and temperature result in an environment where liquid water is not stable, and the lack of a thick atmosphere and significant ozone layer results in a solar ultraviolet (UV) radiation environment that extends down to biologically damaging UV wavelengths of $\sim$200 nm (e.g. Cockell *et al.* 2000; Patel *et al.* 2004). In addition, the ionizing radiation field produced by the unshielded flux of energetic cosmic rays is also destructive to the complex molecules of life (Baumstark-Khan & Facius 2001; Dartnell 2011) and extends metres into the Martian subsurface, far deeper than UV penetration (Pavlov *et al.* 2002; Dartnell *et al.* 2007a, b). These factors, among others, mean that the surface of Mars presents a challenging environment for life to persist. In spite of the harsh exposed surface environment, potential microniche refuges for microbial life, offering protection against the unfiltered solar UV radiation and oxidizing conditions, include cryptoendolith communities within fractures or pore spaces of surface rocks (Friedmann 1986; Wynn-Williams & Edwards 2000), polar ice deposits (Cordoba-Jabonero *et al.* 2005) or deeper in the near-surface regolith. Only a few millimetres of dust coverage is required to screen the damaging UV irradiation to survivable levels (e.g. Cockell & Raven 2004) and numerous studies have been performed on the viability of various microorganisms in the Martian surface environment (see Olsson-Francis & Cockell (2010) for a review), but once exposed to the unshielded UV flux photolytic destruction can be rapid. This study extends this body of work by investigating the detection window for specific biosignatures once previously shielded samples have become exposed to solar UV on the Martian surface during probe operations.

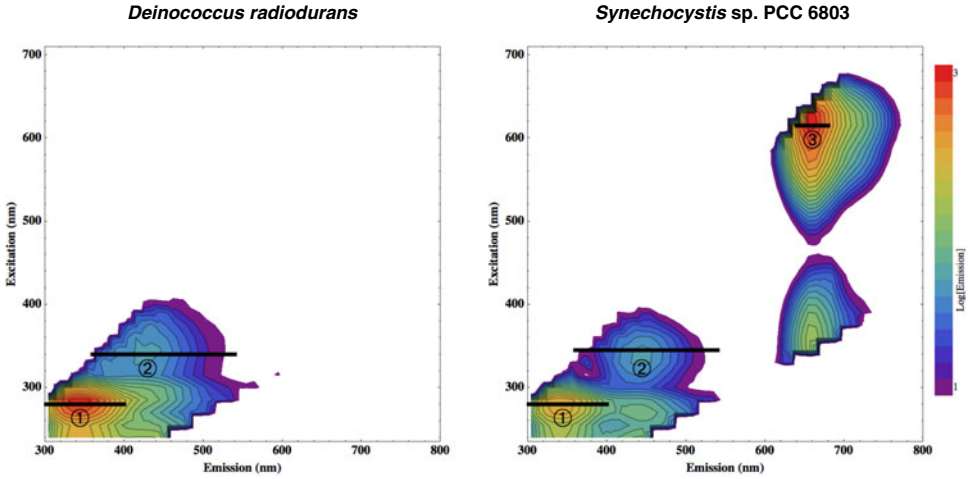

Fig. 1. Excitation–emission matrices (EEMs) representing the full fluorescence response across a broad range of wavelengths for both model organisms studied here, the polyextremophile *Deinococcus radiodurans* (left) and the cyanobacterium *Synechocystis* sp. PCC 6803 (right). Fluorescence intensity is in arbitrary units and colour-coded on a log-10 scale as indicated. Horizontal black bars indicate the spectral ranges analysed to quantify the degradation of signal intensity of different cellular fluorophores with exposure to UV. Cellular fluorophores are labelled as follows: (1) tryptophan; (2) pool of small cellular fluorophores including NAD(P)H; (3) photosynthetic pigments, including chlorophyll and phycocyanin.

Instruments designed to detect organic molecules or other potential tracers of life on Mars include gas chromatography mass spectrometry (GCMS), as installed aboard NASA's Mars Science Laboratory (Mahaffy *et al.* 2012) and proposed for the ESA-Roscosmos ExoMars rover (Evans-Nguyen *et al.* 2008; Goesmann *et al.* 2009); Raman spectroscopy (Ellery & Wynn-Williams 2003; Jorge Villar & Edwards 2006; Marshall & Olcott Marshall 2010; Rull *et al.* 2010), and antibody-based systems such as the Life Marker Chip (Sims *et al.* 2005). Such instrumentation can offer very high sensitivity and discriminatory power, but often requires sample preparation, long exposure times or limited resources or reagents.

It has been proposed therefore to use a complementary instrument based on exciting native autofluorescence from Martian organic compounds, or biomolecules within microorganisms, to rapidly survey potential target regions or triage samples before scrutiny with more discriminatory instruments (Griffiths *et al.* 2008; Storrie-Lombardi *et al.* 2008, 2009; Weinstein *et al.* 2008; Muller *et al.* 2009; Dartnell *et al.* 2010, 2011, 2012). Such an instrument could employ either UV laser diodes for remote detection or UV LEDs with a close-up imager (such as the Mars hand lens imager, MAHLI, aboard Mars Science Laboratory, which has two 365 nm LEDs for UV illumination at night; Edgett *et al.* 2009).

Fluorescence-based detection systems have proved themselves to be sensitive and discriminatory, and have been used in many terrestrial applications. These include the assessment of pollution (JiJi *et al.* 1999; Ko *et al.* 2003; Alberts & Takács 2004; Cory and McKnight 2005) and identification of potentially pathogenic or toxic microorganisms in environmental water or food preparation (Patra & Mishra 2001; Hua *et al.* 2007; Sohn *et al.* 2009; Ziegmann *et al.* 2010). Of most direct relevance here, fluorescence systems have successfully detected trace biomolecules or microbial life in the Atacama desert (Weinstein *et al.* 2008), Antarctic sandstone (Nadeau *et al.* 2008), and glacial (Rohde & Price 2007) and Antarctic ice (Storrie-Lombardi & Sattler 2009).

Excitation-emission matrices

The fluorescence response from a target can be quantitatively described by the generation of an excitation–emission matrix (EEM). Briefly, an EEM is created by recording the fluorescent emission spectrum from an experimental sample across a range of excitation wavelengths, and plotting the fluorescence intensity produced at each excitation–emission (ex–em) wavelength combination as a contour map.

Figure 1 displays the EEMs generated for the two model organisms considered here. *Deinococcus radiodurans* (left) is selected as a polyextremophile able to tolerate high ionizing radiation doses (such as from the cosmic ray flux on to the unshielded Martian surface), and *Synechocystis* sp. PCC 6803 (right) is taken as a model cyanobacterium exhibiting the same cellular fluorophores as cryptoendolith organisms inhabiting UV-shielded microniches. Such representations of the full fluorescence response of microorganisms clearly exhibit different fluorophores within the cell, appearing as fluorescence features at particular ex–em locations within the parameter space. The intense feature was seen at UV wavelengths, with a peak ex–em pairing of about 280–340 nm and labelled (1) in Fig. 1, is due to the amino acid tryptophan bound within cellular proteins (e.g. Ammor 2007).

Both *Deinococcus* and *Synechocystis* also exhibit weaker fluorescence at an ex–em pairing of about 340–450 nm, labelled (2) in the EEMs, which is generally attributed to a

https://doi.org/10.1017/S1473550413000335 Published online by Cambridge University Press

mixed pool of cellular fluorophores including the metabolic coenzymes NADH and NADPH (Ammor 2007). In addition, *Synechocystis* exhibits two broad, intense fluorescence features with a peak emission at about 660 nm, labelled (3). This is fluorescence of the cyanobacterial photosynthetic system for efficiently gathering light and transducing this energy into growth. The photopigment chlorophyll and phycocyanin, a component of the phycobilisome molecular complex that aids light-gathering, are both intrinsically highly fluorescent due to their biological function (Keränen *et al.* 1999).

The horizontal black lines marked in Fig. 1 indicate the spectral regions of interest for following the degradation of these cellular fluorophores by exposure to UV radiation. These are the excitation wavelengths selected for the most sensitive detection of each fluorescent feature, and the width of each bar indicates the emission wavelength range of the spectra plotted in Fig. 4.

Rationale

Here, we expand on recent work (Storrie-Lombardi *et al.* 2008, 2009; Muller *et al.* 2009; Dartnell *et al.* 2010, 2011, 2012) on the utilization of fluorescence for surveying for Martian organics or organisms. These recent studies have demonstrated the feasibility of detecting autofluorescence of polycyclic aromatic hydrocarbons (PAHs) on mineral grains using 365 nm LED (Storrie-Lombardi *et al.* 2008) or 375 nm laser diode (Muller *et al.* 2009) excitation sources and calculated the detection limit to be about 20–145 ppm using the PanCam filter wheel (Storrie-Lombardi *et al.* 2009). The photolytic degradation half-life of these representative PAHs, once uncovered by probe operations, has been experimentally determined to between 25 and 60 h of noontime summer irradiation (Dartnell *et al.* 2012). Biological work has focused on characterizing the complete fluorescence response from different extremophilic and photosynthetic microorganisms to identify the best excitation and emission wavelengths for an instrument (Dartnell *et al.* 2010) and the rate of loss of the fluorescence biosignature from cyanobacteria exposed to ionizing radiation, such as from unshielded cosmic rays on the Martian surface (Dartnell *et al.* 2011). The present study builds on this existing body of knowledge to now look at the rate of degradation of fluorescence signal from model microorganisms exposed unfiltered solar UV radiation.

In order to have survived until the present day, localizations of Martian organics or organisms must have been protected from solar UV and so a Mars exploration probe would need to examine freshly exposed material. A rock abrasion tool (RAT) such as carried by the Mars Exploration Rovers Spirit and Opportunity (Gorevan *et al.* 2003), the rock coring drill on Mars Science Laboratory (Okon 2010) and the 2 m subsurface drill proposed for ExoMars (Vago *et al.* 2006) are all appropriate devices for this. Once exposed to the unfiltered solar UV spectrum on the Martian surface, however, any potential fluorophores will be readily photodegraded and their fluorescence signal lost.

So the key question for the functionality of such a fluorescence-based technique is: on what timescale are the emission signals of different fluorescent targets destroyed by solar UV once uncovered? What is the window of opportunity for detection by instrumentation aboard a rover? In the longer term, the fluorescence-based detection of ice-bound organisms may have significance for the rapid testing of ice profiles for cryoperserved microbial life in the Europan ice shell.

In this study, we expose frozen thin samples of two model microorganisms, the polyextremophile *D. radiodurans* and the cyanobacterium *Synechocystis* sp. PCC 6803, to broad-spectrum UV radiation in a Mars simulation chamber. The changes to the cellular fluorescence response are quantified after total fluences calibrated to between 0.25 and 64 h of equatorial noontime Martian sunlight, and thus the window of opportunity for detection for a fluorescence-based instrument is assessed.

Methods

Cell cultures

Deinococcus radiodurans

The 200 ml of Tryptone digest, Glucose, Yeast extract (TGY) broth in a 1 l conical flask was inoculated with starter culture and incubated at 30 °C with constant agitation at 200 rpm for 44 h to culture until mid-late log phase. The nutrient growth medium TGY is itself fluorescent and so the cell culture was washed by centrifugation and resuspension of the pellet in phosphate buffer solution (PBS; Difco) which is non-fluorescent (Dartnell *et al.* 2010).

Synechocystis sp. PCC 6803

100 ml of BG11 growth medium (Castenholz 1988) in a 1 l conical flask was inoculated with starter culture and incubated for 3 days at 25 °C with constant agitation of 130 rpm in a photosynthesis incubator (Innova 4340, New Brunswick Scientific, St. Albans, UK) providing a photon flux of 46 $\mu E\,m^{-2}\,s^{-1}$. Although it had already been determined that the BG11 growth medium produces no fluorescent emission of its own (Dartnell *et al.* 2010), the culture was centrifuged and resuspended in PBS to allow dilution to the target cell density, as described below.

Sample preparation

The target OD_{600} for optimal measurement of fluorescence of a cell suspension using the spectrofluorimeter instrument described below had been found previously to be around 0.5 (Dartnell *et al.* 2010), representing a compromise between sufficient fluorophore concentration and minimization of scattering or self-shielding by higher cell densities. Cell samples of 1 ml were to be exposed to UV, whereas the quartz spectroflourimeter cuvette is 3 ml, so the *Deinococcus* and *Synechocystis* master cell suspensions were both made to three times the final target OD_{600} of 0.5.

Approximately 1 ml samples of the prepared cell suspension were pipetted into 35 mm diameter (× 10 mm depth) tissue culture dishes. This volume and dish diameter selection results in a sample depth of only 1 mm, avoiding the problem of

https://doi.org/10.1017/S1473550413000335 Published online by Cambridge University Press

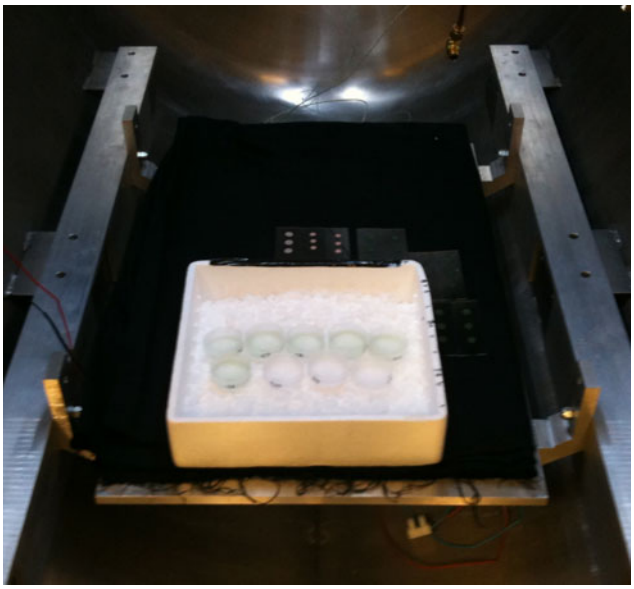

Fig. 2. Photograph of the setup of the experimental exposure. Very thin layers of frozen cell suspensions within tissue culture dishes rest on a bed of dry ice, to emulate Martian surface temperatures, within the Mars simulation chamber at the Open University. The UV irradiation lamp is not yet switched on in this image.

self-shielding during UV irradiation. The absorption coefficient of water over the wavelength range 185–400 nm is negligible (Warren 1984) and so the UV exposure is uniform through the 1 mm depth. Cell samples were frozen to −80 °C before transportation on dry ice to the Mars simulation chamber. Control samples were prepared and transported identically to the test samples, but not exposed to UV radiation in the Mars simulation chamber.

UV irradiation

Cell sample dishes were laid flat on a bed of dry ice to maintain a temperature of −80 °C (representative of the Martian surface) throughout irradiation and arranged in the Mars simulation chamber, as shown in Fig. 2.

The xenon lamp used in this study produced a UV emission spectrum closely matching that modelled for the unfiltered sunlight incident on the Martian equatorial surface at noon during northern summer (Ls = 90°) and nominal atmospheric dust loading (Patel *et al.* 2002). The flux rate is also calibrated to be ten times greater to allow accelerated irradiations, and so to create Martian equivalent exposures of 0.25, 0.5, 1, 2, 4, 8, 32 and 64 h, real-time durations of 1.5 min, 3 min, 6 min, 12 min, 24 min, 48 min, 3 h 12 min, and 6 h 24 min, respectively, were employed. See Dartnell *et al.* (2012) for further details on the irradiation spectrum. This distribution of dose levels was designed to allow for detailed observation of the effects through low exposures while also providing results on the response after much greater irradiation. This data coverage over a wide scale proved to be very effective in revealing, for example, the complex behaviour of the 448 nm emission feature of *Synechocystis* (shown in Fig. 5, solid green line). Thus, the experimental procedure reproduced Martian surface temperature and irradiation spectrum, but was conducted at ambient atmospheric conditions. Photolytic chemistry and thus biomolecule destruction from UV radiation is temperature-dependent, but not affected by pressure *per se* at the molecular level, and so the Martian low atmospheric pressure was not experimentally recreated in order to remove sublimation of the ice samples as a confounding factor for fluorescence degradation.

Fluorescence analysis

Immediately before analysis, the 1 ml cell samples were thawed, diluted in 2 ml of PBS to the optimum OD_{600} of 0.5, and pipetted into a 3 ml UV-C quartz cuvette (Fisher, Loughborough, UK) cleansed with 70% ethanol and which yields no background fluorescence of its own.

Fluorescent emission of samples was measured with a Perkin Elmer LS55 fluorescence spectrometer (Perkin Elmer, Cambridge, UK), which consists of a pulsed xenon arc lamp light source, excitation and emission scanning monochromators, a sample compartment with cuvette holder, and a photomultiplier tube detector.

Emission spectra were recorded between 300 and 800 nm, with an excitation slit width of 8 nm and emission slit width of 5 nm, and data points logged every 0.5 nm at a scan speed of 1000 nm min^{-1}. The excitation wavelength was incremented in 15 nm steps between 240 and 705 nm, which produced a total of 32 emission spectra for each sample. Thus, the complete fluorescence dataset collected for each sample represents a three-dimensional datacube of emission intensity measurements at 32 000 ex–em wavelength combinations. To smooth the recorded emission spectra and reduce the computational demands required for subsequent processing and plotting of the complete EEM, emission spectra were averaged into bins 10 nm wide.

Excitation–emission matrices were generated from the acquired datacube by data transformation and analysis computer code written by the lead author in Mathematica 9.0 (Wolfram Research, Champaign, USA). Each fluorescence profile (for example, in Figs. 1 and 3) is presented on a log-10 intensity scale and displayed with rainbow colour coding and 20 contour lines. The appropriate range for colour coding of the fluorescence intensity was determined from the emission intensity histogram, as explained in Dartnell *et al.* (2010). The error in determining the peak height of the selected fluorescence features from the emission spectra is estimated to be no more than 5%.

Results

Figure 3 displays the complete dataset acquired for the full fluorescence response of the two microorganisms studied here, *D. radiodurans* and *Synechocystis* sp. PCC 6803. All EEMs are plotted over the same spectral region (excitation wavelength between 240 and 700 nm; emission wavelength between 300 and 800 nm) and using the same colour-coded log-scale of emission intensity, spanning two orders of magnitude.

https://doi.org/10.1017/S1473550413000335 Published online by Cambridge University Press

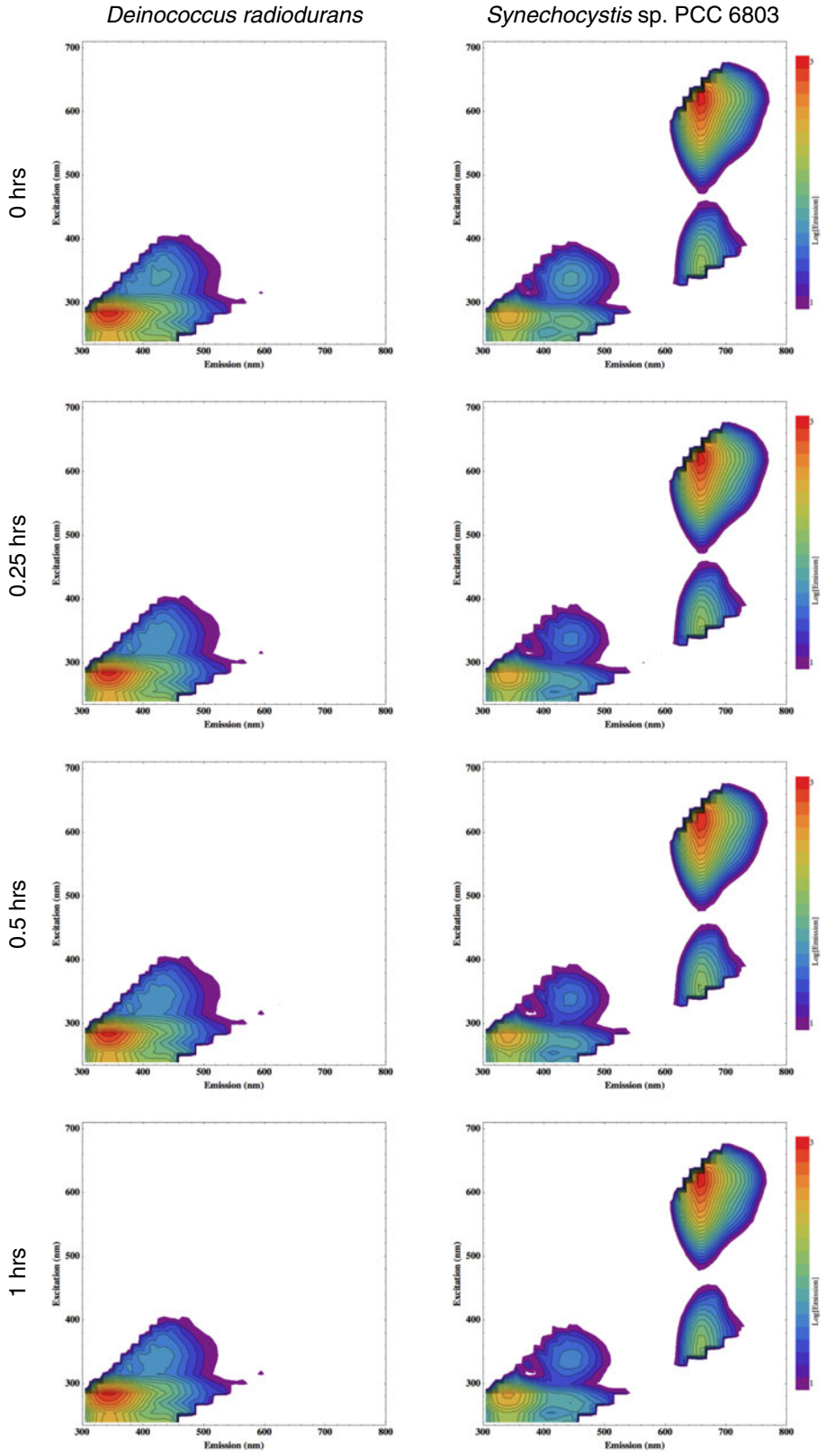

Fig. 3. The complete EEM dataset acquired on the fluorescence response of the two model organisms after increasing UV irradiation. Emission intensity is in arbitrary units and colour-coded on a log-10 scale as indicated. The total UV doses used are calibrated to the equivalent number of hours of exposure on the Martian surface, calculated for equatorial noontime conditions (Patel *et al.* 2002): 0.25, 0.5, 1, 2, 4, 8 and a maximum of 32 h Mars-equivalent exposure for *Deinococcus* and 64 h for *Synechocystis*. Minimal degradation of fluorescence signal is observed for *Deinococcus*, but the cyanobacterium exhibits noticeable diminishment of photosystem fluorescence (peaking at an excitation–emission wavelength pairing of about 615–660 nm) and a stark increase in the fluorescent feature at an ex–em pairing of about 340–440 nm.

https://doi.org/10.1017/S1473550413000335 Published online by Cambridge University Press

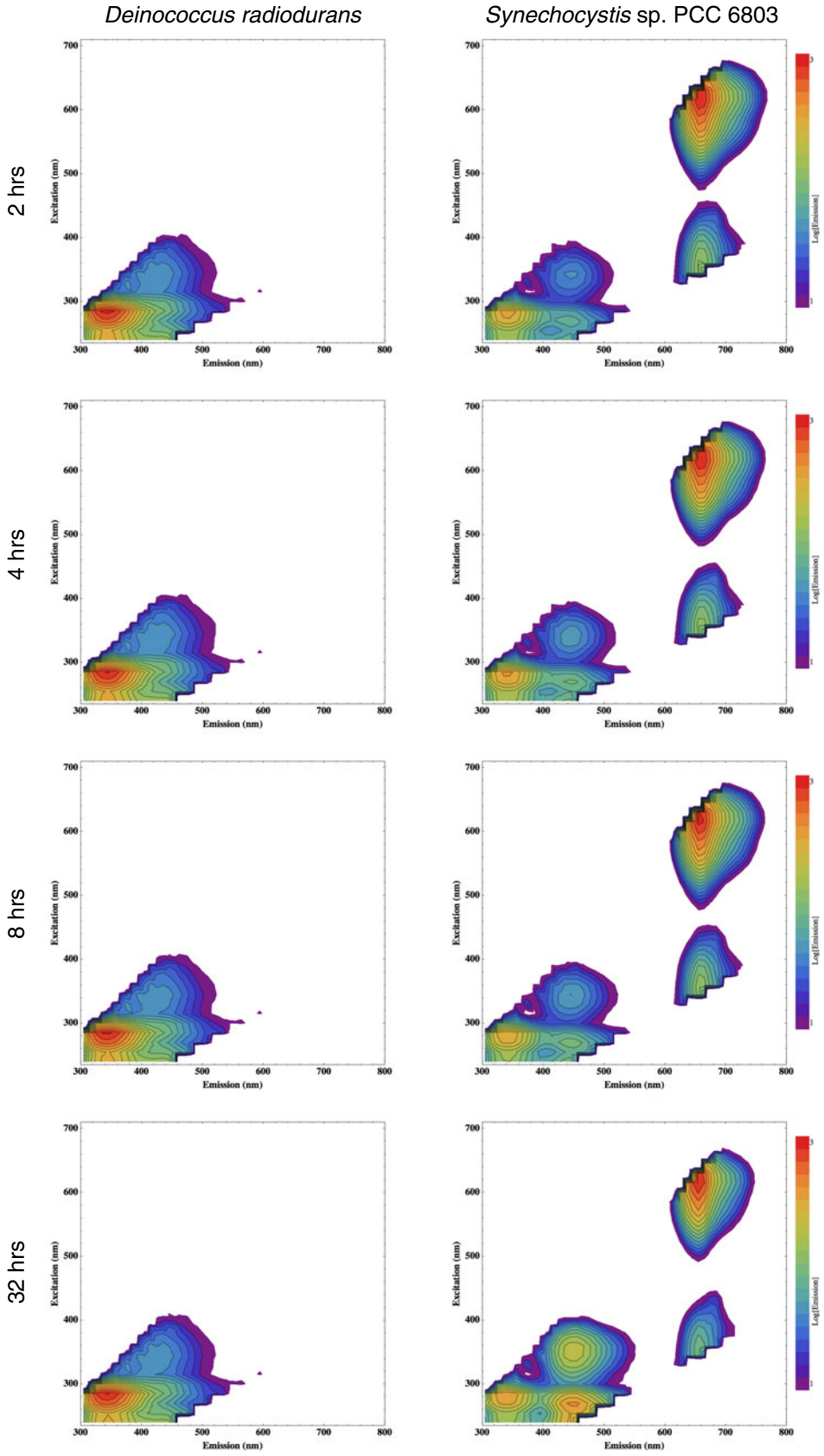

Fig. 3. Continued.

https://doi.org/10.1017/S1473550413000335 Published online by Cambridge University Press

Complete EEMs were generated for each UV exposure, rather than only measuring spectra covering the fluorescent features of interest (as indicated in Fig. 1 with horizontal black lines) to enable the detection of any shifting of peak excitation or emission wavelength or appearance of new fluorescent features with irradiation.

While there are no immediately obvious changes in the EEMs generated for *D. radiodurans* exposed to increasing doses of UV radiation, differences are apparent in the irradiated *Synechocystis* cells. The height of the intense fluorescent peak centred on an ex–em pairing of about 600–660 nm (labelled (3) in Fig. 1), produced by chlorophyll and phycocyanin associated with the cyanobacterial thylakoid membrane for photosynthesis, can be seen to diminish with increasing exposure. Even more notable is the stark increase in fluorescence of the feature at an ex–em pairing of about 340–450 nm (labelled (2) in Fig. 1).

These fluorescent features are shown in greater spectral detail in Fig. 4. For each fluorescent feature, the optimal excitation wavelength is selected (280 nm, 340 or 345 nm and 615 nm) and the corresponding emission spectrum plotted over the wavelength range indicated in Fig. 1. Fluorescence spectra recorded after Martian equivalent UV exposures of 0 (the control samples), 0.25, 0.5, 1, 2, 4, 8 and 32 h (in the case of *Deinococcus*) or 64 h (in the case of *Synechocystis*) are stacked on the same axes and colour-coded from light-grey to black to indicate longer duration of exposure, to enable comparison of the remaining emission intensity after exposure to increasing UV irradiations. The peak of fluorescent emission determined in these spectra is indicated with a green line, and labelled with the wavelength for clarity.

Both *Deinococcus* and *Synechocystis* exhibit a peak in protein-bound tryptophan fluorescence (280 nm excitation; top row) at 342 nm, and the peak emission from the cyanobacterial light-harvesting machinery (bottom pane), which is dominated by chlorophyll and phycocyanin, occurs at 658 nm.

Figure 4 also reveals a spectral characteristic not readily apparent in the full contour-mapped EEMs shown in Fig. 3. The fluorescent feature emitting between about 400 and 500 nm from excitation at about 340 nm seems to be a symmetrical peak in the EEMs (labelled (2) in Fig. 1), but is clearly shown in Fig. 4 (middle row) to be composed of two distinct peaks. These are labelled in Fig. 4 to exhibit emission peaks at 387 and 425 nm for *Deinococcus* and 394 and 448 nm for *Synechocystis*. The *Synechocystis* emission spectra (Fig. 4: middle row, right) are plotted on an extended intensity scale on the *y*-axis, which clearly shows that this 448 nm fluorescence feature rises to twice (205%) that of the initial intensity after 64 h Mars equivalent hours of UV irradiation.

The peak intensities of each of these fluorescence features, taken at the wavelength indicated, are extracted from these emission spectra and normalized to the initial value as 100% fluorescence signal intensity. Figure 5 plots these results, quantifying the change in fluorescence signal intensity of different cellular fluorophores as a function of increasing UV exposure.

Discussion and conclusions

Degradation of tryptophan and photosystem fluorescence

Figure 5 shows that, while there is experimental scatter of the data points of about ±5%, all three fluorescence features exhibited by *Deinococcus* (dashed lines) behave similarly in the long-term trend, declining to about 90% of the initial intensity after the maximum exposure of 32 Mars equivalent hours employed in this study. Colonies of *Deinococcus* are brightly coloured due to their expression of six carotenoid pigments related to β-carotene (Carbonneau *et al.* 1989), the dominant of which is deinoxanthin (Lemee *et al.* 1997). Such carotenoids offer UV photoprotection by quenching oxygen-free radicals produced by short-wavelength irradiation and possibly also by directly screening the UV light (Cockell & Knowland 1999), and so the cellular fluorophores within *Deinococcus* are well shielded from photodegradation.

By comparison, the tryptophan signal intensity in *Synechocystis* (labelled (1) in Figs. 1 and 4) is much more sensitive to UV photodegradation than the corresponding feature in *Deinococcus*. Figure 5 shows tryptophan fluorescence (solid purple line) to have been reduced to 80% after 8 h and only 50% after 64 h.

The signal most readily degraded by UV irradiation is fluorescence of the photosynthetic pigments (labelled (3) in Figs. 1 and 4) – diminished to only 35% after 64 h exposure. This can be expected as the biological function of these molecules is to optimize the harvesting of light energy and so they are readily photobleached (an effect also studied by Sinha *et al.* 2002). UV-B radiation (280–315 nm) is known to damage photosynthetic pigments, and the previous work has shown that the accessory biliproteins in the phycobilisome (such as phycocyanin) are bleached first, followed by carotenoids and chlorophyll damaged last (Sinha *et al.* 1995). Ultraviolet radiation also causes structural destruction of the phycobilisome complex that enhances light collection in photosynthesis. The first step in the breakdown of phycobilisomes is probably the destruction of linker proteins, with degradation products forming as components of the phycobilisome are broken down into hexamers, trimers and then monomers (Banerjee *et al.* 1998).

The loss of photosystem fluorescence found here, with a decrease of around 20% from the initial signal intensity after 8 h of simulated Martian flux, is less than that reported by a similar study working with dried monolayers of the desiccation-resistant cyanobacterium *Chroococcidiopsis* sp. 029. Cockell *et al.* (2005) found that autofluoresence of the cyanobacteria photosynthetic apparatus (emission > 590 nm) was reduced to 14% of the initial intensity after one hour Martian equivalent exposure, and to 5% after 4 h. This greater degradation may be due to irradiation in a monolayer, which may indicate a synergistic destructive effect of cellular dehydration coupled with UV radiation, or a protective effect for our cells irradiated at very low temperature (−80 °C, representative of the Martian surface).

https://doi.org/10.1017/S1473550413000335 Published online by Cambridge University Press

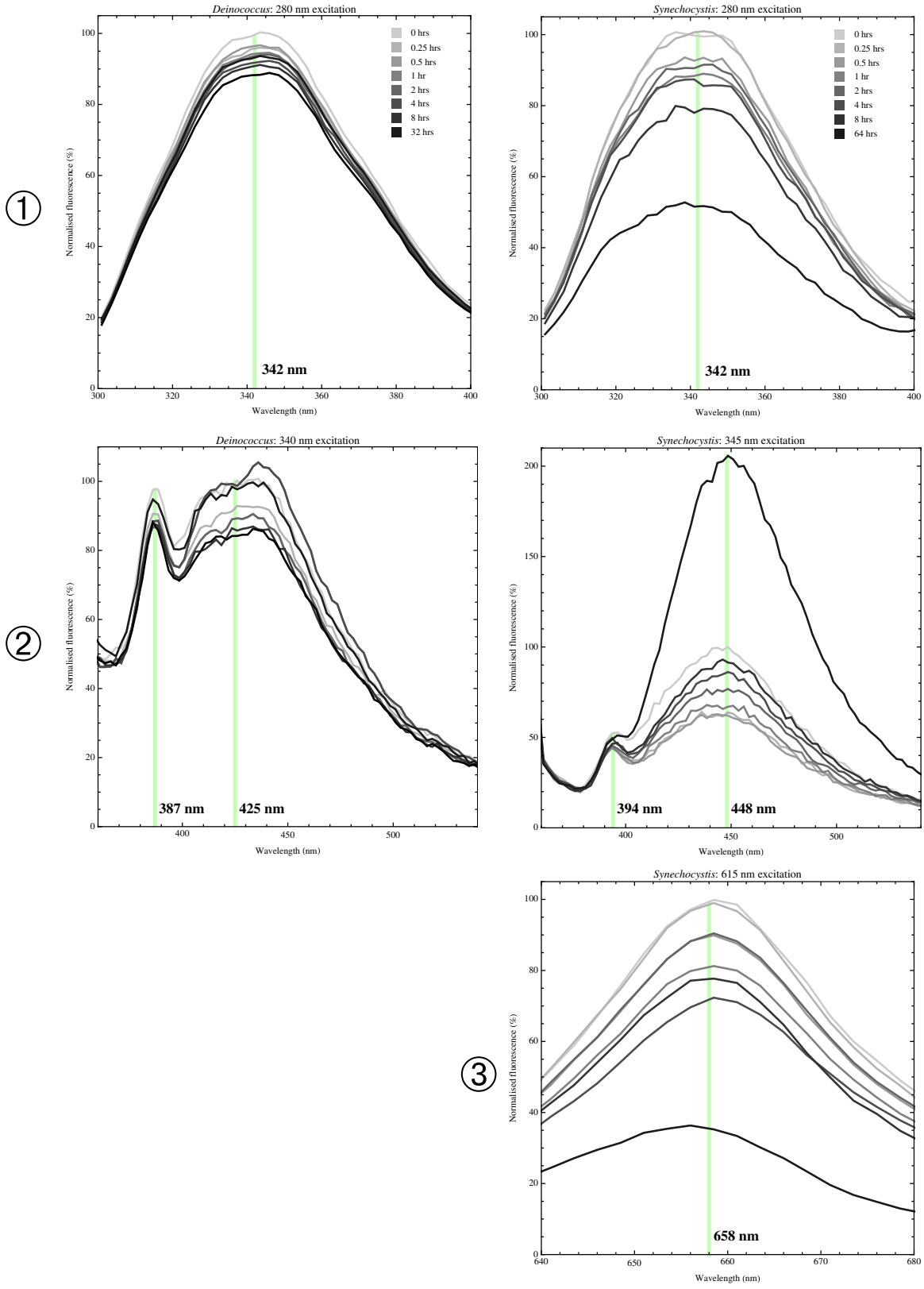

Fig. 4. Stacked fluorescence emission spectra centred on the regions of interest, as indicated in Fig. 1: (1) tryptophan; (2) pool of small cellular fluorophores including NAD(P)H; (3) photosynthetic pigments, including chlorophyll and phycocyanin. Spectra are colour-coded to increasing UV exposure from light grey to black. The peak of each fluorescence feature quantified in this study is indicated by the vertical green line, with the wavelength labelled. The decline in remaining fluorescence from tryptophan (280 nm excitation) and the photosystem (615 nm excitation) of *Synechocystis* is clearly seen in these plots, and the fluorescence feature elicited by excitation at about 340–345 nm (middle row) in both organisms is revealed to be composed of two distinct peaks.

https://doi.org/10.1017/S1473550413000335 Published online by Cambridge University Press

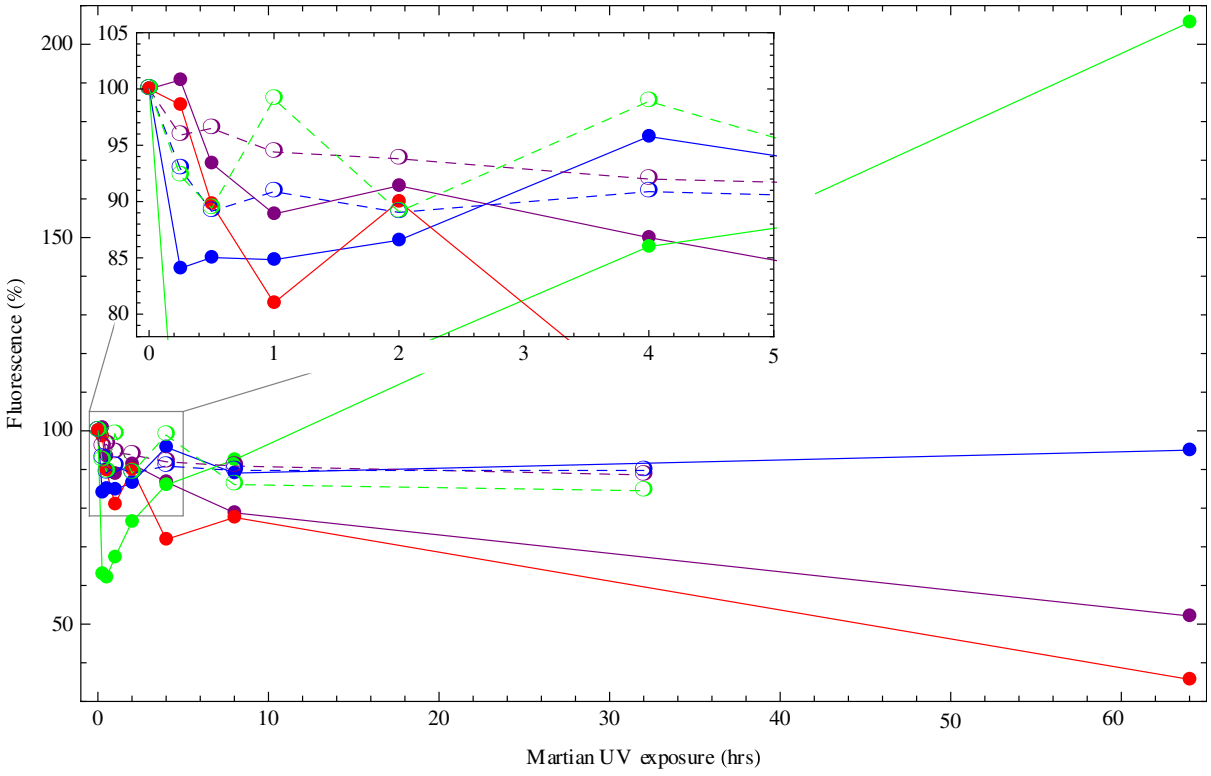

Fig. 5. Change in emission intensity of cellular fluorophores as a function of hours of UV exposure on the Martian surface for *Deinococcus* (dashed) and *Synechocystis* (solid). Fluorescence profiles are colour-coded to the peak emission wavelength, as labelled on Fig. 4: 342 nm tryptophan fluorescence (purple); 387/394 nm emission of *Deinococcus*/*Synechocystis* (blue); 425/448 nm emission of *Deinococcus*/*Synechocystis* (green); 658 nm emission from the *Synechocystis* photosystem (red).

Response of cyanobacterial 448 nm emission feature

The behaviour of the *Synechocystis* fluorescence observed when exciting at about 345 nm (Fig. 4, middle right) is more complex and interesting. As discussed already, although the feature at an ex–em pairing of about 350–450 nm appears in the EEM representations in Fig. 1 (labelled (2)) and Fig. 3 to be a symmetrical peak; it is revealed by the emission spectra in Fig. 4 to in fact be composed of two distinct peaks.

These two peaks are roughly equivalent in *Deinococcus* (Fig. 4, middle left), whereas the ratio in *Synechocystis* between the intensity of the shorter wavelength emission peak (394 nm) and the longer wavelength peak (448 nm) varies substantially with UV exposure. The 394 nm peak is shown in Fig. 5 (solid blue line) to remain relatively unaffected by even the highest UV exposure level and retains a signal intensity closely comparable with the *Deinococcus* cellular fluorophores (dashed lines). The 448 nm emission peak, however, exhibits a far more complex behaviour in response to UV irradiation (solid green line in Fig. 5). Fluorescence intensity drops rapidly to 60% of the initial value after only brief UV exposure, before steadily rising again. Fluorescence exceeds the initial value (100%) after roughly 12 h of Mars equivalent exposure and continues to increase to twice the original emission after 64 h irradiation.

The spectral characteristics of this fluorescence feature, with an ex–em pairing close to 340–450 nm, and the feature emitting at the same wavelength (located below the label (2) in Fig. 1), with ex–em pairing of 260–450 nm, correspond to those of NADH and NAD+, respectively. Although these are ubiquitous co-enzymes involved in redox metabolism in the cell, they are not thought to be responsible for the shifts in fluorescence seen in the irradiated cyanobacteria. NADH and NAD+ are the reduced and oxidized forms of the same coenzyme and so cannot account for an increase in fluorescence at both of these ex–em pairings simultaneously, as is observed in the irradiated cyanobacteria (Fig. 3).

Instead, the profile of 448 nm emission (Fig. 4, solid green line) is interpreted here as representing an initial rapid photobleaching of the fluorescence of an original pool of cellular fluorophores (up until between half an hour and 1 h of exposure), followed by an accumulation of fluorescent break-down products generated by the photolytic destruction of cellular molecules by the short wavelength UV radiation.

These accumulating fluorescent break-down products are believed to be derived from chlorophyll, a major component of the cyanobacterial cell. The spectral properties of this feature (label (2) in Fig. 1), peaking at an ex–em pairing of 345–448 nm, match that of the fluorescent chlorophyll catabolites (FCCs) that show peak fluorescence at 450 nm after excitation at 350 nm, and are produced by the metabolic degradation pathways within ripening bananas (Moser *et al.* 2008, 2009), senescent banana leaves (Banala *et al.* 2010) and those of the peace lily (Kräutler *et al.* 2010). The shift in

https://doi.org/10.1017/S1473550413000335 Published online by Cambridge University Press

fluorescent emission to shorter wavelengths (blue-shifting), from chlorophyll in healthy cyanobacteria cells at ~685 nm (label (3) in Fig. 1) to these FCCs at ~450 nm is caused by changes to the molecular structure of the fluorophore, such as loss of aromatic rings or a decrease in the number of conjugated bonds in a linear chain (Coble 1996).

The ex–em pairing of these FCCs corresponds very well with that measured here for the anomalously increasing fluorescent feature (labelled (2) in Fig. 1 and seen most prominently in the 64 h EEM in Fig. 3) in UV-exposed cyanobacteria. Thus, it is believed that the stark increase in the ~450 nm emission features after one hour Mars equivalent UV dose (Fig. 4, solid green line) is due to the accumulation of chlorophyll photolytic products. An identical pattern of growing intensity of a fluorescent feature at ex–em pairing about 350–450 nm has also been reported for the exposure of Synechocysis sp. PCC 6803 to increasing doses of gamma-ray ionizing radiation, and was also interpreted as the accumulation of radiolytically produced chlorophyll break-down products (Dartnell *et al.* 2011).

Relevance to Mars probe operations

As discussed in the introduction, exploitation of the autofluorescence of aromatic prebiotic compounds or the biomolecules within microorganisms has been proposed for instrumentation suitable for Mars lander probes. Such devices could offer a critical surveying or triaging function for surface operations, identifying the most promising sites or samples for examination with more time, energy or time- and resource-intensive analytical techniques such as GCMS.

For the successful design and operation of such a fluorescence-based instrument, it is important to determine the most effective excitation and emission wavelengths, as well as the response of the fluorescent target molecules once they have been extracted from their protected location beneath the surface and exposed to the intense UV component of the unfiltered sunlight on Mars. The key question is: does the irradiated fluorescence signal persist over the timescales required for robotic probe operations to enable detection?

Recent work has studied the UV photolytic degradation of the fluorescence signal from key prebiotic compounds, PAHs (Dartnell *et al.* 2012), and here we have extended this work to the fluorescent biosignature of microorganisms.

The native fluorescence of the polyextremophile *D. radiodurans*, once exposed to the unfiltered Martian sunlight, has been found here to be stable over an appreciable period of time. Figure 4 shows only 10% decrease in the signal strength after an UV exposure equivalent to 32 h of continuous Martian equatorial noon solar flux.

A cyanobacterium, such as *Synechocystis* sp. PCC 6803, without significant quantities of UV-shielding compounds such as mycosporine-like amino acids or scytonemin, exhibits significant photobleaching of the fluorescence signal from tryptophan and the photosynthetic molecules chlorophyll and phycocyanin by UV irradiation. This study found 20% signal loss from these fluorophores after only 8 h.

These durations represent a conservative estimate as cells emplaced in an environmental setting, embedded within a mineral matrix or partially protected by dust, would receive additional UV shielding. Furthermore, these Mars-equivalent UV fluxes are calculated from a model for equatorial midday sun during northern summer (Ls = 90°) and nominal atmospheric dust loading (Patel *et al.* 2002), and so represent a relatively high level of dose rate. At increasing latitudes or time in the seasonal cycle, the actual UV flux experienced would be lower. More importantly, the instantaneous UV flux varies during the Martian day as the sun arcs through the sky, and undergoes increasing scattering effects from the atmosphere. Taking this time variation into account and integrating across a complete diurnal cycle reveals that every hour of Mars equivalent exposure used here equates to 0.16 sols (Dartnell *et al.* 2012).

Thus, *Deinococcus* autofluorescence remains at roughly 90% of the initial, unexposed intensity, and the *Synechocystis* tryptophan and photosystem signal at around 65%, over five to six Martian sols. This is a meaningful window of opportunity in the timescale of robotic surface operations and indicates that such fluorescence biosignatures of current life could indeed persist for long enough to be detectable after exposure to the Martian UV radiation.

The detectability of the components of previously protected cyanobacteria would even appear to be enhanced over these timescales due to the increase in fluorescence intensity of the 448 nm emission feature, believed to be due to the accumulation of photolytic breakdown products.

Acknowledgements

LRD was supported by the UCL Institute of Origins Post-Doctoral Research Associateship. MRP was supported by funding from the Science and Technology Facilities Council (STFC).

References

Alberts, J. & Takács, M. (2004). Comparison of the natural fluorescence distribution among size fractions of terrestrial fulvic and humic acids and aquatic natural organic matter. *Organ. Geochem.* **35**(10), 1141–1149.

Ammor, M. (2007). Recent advances in the use of intrinsic fluorescence for bacterial identification and characterization. *J. Fluoresc.* **17**(5), 455–459.

Banala, S., Moser, S., Müller, T., Kreutz, C., Holzinger, A., Lütz, C. & Kräutler, B. (2010). Hypermodified fluorescent chlorophyll catabolites: source of blue luminescence in senescent leaves. *Angew. Chemi. Inter. Ed.* **49**(30), 5014.

Banerjee, M., Sinha, R.P. & Hader, D.-P. (1998). Biochemical and Spectroscopic Changes in Phycobiliproteins of the Cyanobacterium, Aulosira fertilissima, induced by UV-B Radiation. *Acta Protozool.* **37**(3), 145–148.

Baumstark-Khan, C. & Facius, R. (2001). Life under Conditions of Ionizing Radiation. *Astrobiol., Quest Cond. Life* 260–283.

Carbonneau, M., Melin, A., Perromat, A. & Clerc, M. (1989). The action of free radicals on *Deinococcus radiodurans* carotenoids. *Arch. Biochem. Biophys.* **275**(1), 244–251.

https://doi.org/10.1017/S1473550413000335 Published online by Cambridge University Press

Castenholz, R. (1988). Culturing methods for cyanobacteria. *Methods Enzymol*. **167**, 68–93.

Coble, P. (1996). Characterization of marine and terrestrial DOM in seawater using excitation-emission matrix spectroscopy. *Mar. Chem*. **51**(4), 325–346.

Cockell, C. & Knowland, J. (1999). Ultraviolet radiation screening compounds. *Biol. Rev*. **74**(3), 311–345.

Cockell, C. & Raven, J. (2004). Zones of photosynthetic potential on Mars and the early Earth. *Icarus* **169**(2), 300.

Cockell, C., Schuerger, A., Billi, D., Friedmann, E. & Panitz, C. (2005). Effects of a simulated Martian UV flux on the Cyanobacterium, Chroococcidiopsis sp. 029. *Astrobiology* **5**(2), 127–140.

Cockell, C., Catling, D.C., Davis, W.L., Snook, K., Kepner, R., Lee, P. & Mckay, C.P. (2000). The Ultraviolet Environment of Mars: Biological Implications Past, Present, and Future. *Icarus* **146**, 343–359.

Cordoba-Jabonero, C., Zorzano, M., Selsis, F., Patel, M. & Cockell, C. (2005). Radiative habitable zones in Martian polar environments. *Icarus* **175**(2), 360–371.

Cory & McKnight (2005). Fluorescence Spectroscopy Reveals Ubiquitous Presence of Oxidized and Reduced Quinones in Dissolved Organic Matter. *Environmental Science & Technology* **39**(21), 8142–8149.

Dartnell, L.R. (2011). Ionizing radiation and life. *Astrobiology* **11**(6), 551–582.

Dartnell, L.R., Desorgher, L., Ward, J. & Coates, A. (2007a). Modelling the surface and subsurface Martian radiation environment: implications for Astrobiology. *Geophys. Res. Lett*. **34**(2), L02207.

Dartnell, L.R., Desorgher, L., Ward, J.M. & Coates, A.J. (2007b). Martian sub-surface ionising radiation: biosignatures and geology. *Biogeosciences* **4**, 545–558.

Dartnell, L.R., Storrie-Lombardi, M.C. & Ward, J.M. (2010). Complete fluorescent fingerprints of extremophilic and photosynthetic microbes. *Int. J. Astrobiol*. **9**(4), 245–257.

Dartnell, L.R., Storrie-Lombardi, M., Mullineaux, C., Ruban, A., Wright, G., Griffiths, A., Muller, J.-P. & Ward, J. (2011). Degradation of cyanobacterial biosignatures by ionizing radiation. *Astrobiology* **11**(10), 997–1016.

Dartnell, L.R., Patel, M., Storrie-Lombardi, M.C., Ward, J.M. & Muller, J.-P. (2012). Experimental determination of photostability and fluorescence-based detection of PAHs on the Martian surface. *Meteorit. Planet. Sci*. **47**(5), 806–819.

Edgett, K., Ravine, M. & Caplinger, M. (2009). The Mars Science Laboratory (MSL) Mars Hand Lens Imager (MAHLI) Flight Instrument. In *40th Lunar and Planetary Science Conf. (Lunar and Planetary Science XL)*, The Woodlands, Texas, held 23–27 March, 2009, *id.1197*.

Ellery, A. & Wynn-Williams, D. (2003). Why Raman Spectroscopy on Mars? A case of the right tool for the right job. *Astrobiology* **3**(3), 565–579.

Evans-Nguyen, T., Becker, L., Doroshenko, V. & Cotter, R. (2008). Development of a low power, high mass range mass spectrometer for Mars surface analysis. *Int. J. Mass Spectrom*. **278**(2–3), 170–177.

Friedmann, E. (1986). The antarctic cold desert and the search for traces of life on Mars. *Adv. Space Res*. **6**(12), 265–268.

Goesmann, F., Becker, L. & Raulin, F. (2009). MOMA, the search for organics of the ExoMars mission. *EPSC Abstr*. **4**, EPSC2009-624.

Gorevan, S. *et al*. (2003). Rock abrasion tool: Mars exploration rover mission. *J. Geophys. Res*. **108**(E12), 8068.

Griffiths, A., Coates, A., Muller, J.-P., Storrie-Lombardi, M., Jaumann, R., Josset, J.-L., Paar, G. & Barnes, D. (2008). Enhancing the effectiveness of the ExoMars PanCam instrument for astrobiology. *Geophys. Res. Abstr*. **10**, EGU2008-A-09486.

Hua, B., Dolan, F., Mcghee, C., Clevenger, T.E. & Deng, B. (2007). Water-source characterization and classification with fluorescence EEM spectroscopy: PARAFAC analysis. *Int. J. Environ. Anal. Chem*. **87**(2), 135–147.

JiJi, R., Cooper, G. & Booksh, K. (1999). Excitation-emission matrix fluorescence based determination of carbamate pesticides and polycyclic aromatic hydrocarbons. *Anal. Chim. Acta* **397**(1–3), 61–72.

Jorge Villar, S. & Edwards, H. (2006). Raman spectroscopy in astrobiology. *Anal. Bioanal. Chem*. **384**(1), 100–113.

Keränen, M., Aro, E.-M. & Tyystjärvi, E. (1999). Excitation-Emission Map as a Tool in Studies of Photosynthetic Pigment-Protein Complexes. *Photosynthetica* **37**(2), 225–237.

Ko, E., Lee, C., Kim, Y. & Kim, K. (2003). Monitoring PAH-contaminated soil using laser-induced fluorescence (LIF). *Environ. Technol*. **24**(9), 1157–1164.

Kräutler, B., Banala, S., Moser, S., Vergeiner, C., Müller, T., Lütz, C. & Holzinger, A. (2010). A novel blue fluorescent chlorophyll catabolite accumulates in senescent leaves of the peace lily and indicates a split path of chlorophyll breakdown. *FEBS Lett*. **584**(19), 4215–4221.

Lemee, L., Peuchant, E., Clerc, M., Brunner, M. & Pfander, H. (1997). Deinoxanthin: a new carotenoid isolated from *Deinococcus radiodurans*. *Tetrahedron* **53**(3), 919–926.

Mahaffy, P. *et al*. (2012). The sample analysis at Mars investigation and instrument suite. *Space Sci. Rev*. **170**(1–4), 401–478.

Marshall, C. & Olcott Marshall, A. (2010). The potential of Raman spectroscopy for the analysis of diagenetically transformed carotenoids. *Phil. Trans. R. Soc. A, Math. Phys. Eng. Sci*. **368**(1922), 3137–3144.

Moser, S., Müller, T., Ebert, M.-O., Jockusch, S., Turro, N.J. & Kräutler, B. (2008). Blue luminescence of ripening bananas. *Angew. Chem. Int. Ed*. **47**(46), 8954–8957.

Moser, S., Müller, T., Holzinger, A., Lütz, C., Jockusch, S., Turro, N. & Kräutler, B. (2009). Fluorescent chlorophyll catabolites in bananas light up blue halos of cell death. *Proc. Natl. Acad. Sci. USA* **106**(37), 15538–15543.

Muller, J.-P., Storrie-Lombardi, M. & Fisk, M. (2009). WALI – Wide Angle Laser Imaging enhancement to ExoMars PanCam: a system for organics and life detection. *EPSC Abstr*. **4**, EPSC2009-2674-2001.

Nadeau, J., Perreault, N., Niederberger, T., Whyte, L., Sun, H. & Leon, R. (2008). Fluorescence microscopy as a tool for *in situ* life detection. *Astrobiology* **8**(4), 859–874.

Okon, A.B. (2010). Mars Science Laboratory Drill. In *Proc. 40th Aerospace Mechanisms Symp., NASA Kennedy Space Center*, 12–14 May, 2010, p 1–16.

Olsson-Francis, K. & Cockell, C. (2010). Experimental methods for studying microbial survival in extraterrestrial environments. *J. Microbiol. Methods* **80**(1), 1–13.

Patel, M., Zarnecki, J. & Catling, D. (2002). Ultraviolet radiation on the surface of Mars and the Beagle 2 UV sensor. *Planet. Space Sci*. **50**(9), 915–927.

Patel, M., Bérces, A., Kerékgyárto, T., Rontó, G., Lammer, H. & Zarnecki, J. (2004). Annual solar UV exposure and biological effective dose rates on the Martian surface. *Adv. Space Res*. **33**(8), 1247–1252.

Patra, D. & Mishra, A. (2001). Investigation on simultaneous analysis of multicomponent polycyclic aromatic hydrocarbon mixtures in water samples: a simple synchronous fluorimetric method. *Talanta* **55**(1), 143–153.

Pavlov, A., Blinov, A. & Konstantinov, A. (2002). Sterilization of Martian surface by cosmic radiation. *Planet. Space Sci*. **50**(7–8), 669–673.

Rohde, R. & Price, P. (2007). Diffusion-controlled metabolism for long-term survival of single isolated microorganisms trapped within ice crystals. *Proc. Natl. Acad. Sci. USA* **104**(42), 16592–16597.

Rull, F. *et al*. (2010). ExoMars Raman laser spectrometer overview. *Proc. SPIE* **7819**(1), 781911–15.

Sims, M., Cullen, D., Bannister, N., Grant, W., Henry, O., Jones, R., McKnight, D., Thompson, D. & Wilson, P. (2005). The specific molecular identification of life experiment (SMILE). *Planet. Space Sci*. **53**(8), 781–791.

Sinha, R., Richter, P., Faddoul, J., Braun, M. & Hader, D.-P. (2002). Effects of UV and visible light on cyanobacteria at the cellular level. *Photochem. Photobiol. Sci*. **1**(8), 553–559.

Sinha, R.P., Kumar, H.D., Kumar, A. & Hader, D.-P. (1995). Effects of UV-B irradiation on growth, survival, pigmentation and nitrogen metabolism enzymes in cyanobacteria. *Acta Protozool*. **34**(3), 187–192.

Sohn, M., Himmelsbach, D., Barton, F. & Fedorka-Cray, P. (2009). Fluorescence spectroscopy for rapid detection and classification of bacterial pathogens. *Appl. Spectrosc.* **63**(11), 1251–1255.

Storrie-Lombardi, M., Muller, J., Fisk, M., Griffiths, A. & Coates, A. (2008). Potential for non-destructive astrochemistry using the ExoMars PanCam. *Geophys. Res. Lett.* **35**, L12201.

Storrie-Lombardi, M. & Sattler, B. (2009). Laser-Induced Fluorescence Emission (L.I.F.E.): *in situ* nondestructive detection of microbial life in the ice covers of Antarctic Lakes. *Astrobiology* **9**(7), 659–672.

Storrie-Lombardi, M., Muller, J.-P., Fisk, M., Cousins, C., Sattler, B., Griffiths, A. & Coates, A. (2009). Laser-Induced Fluorescence Emission (L.I.F.E.): searching for Mars organics with a UV-enhanced PanCam. *Astrobiology* **9**(10), 953–964.

Vago, J., Gardini, B., Kminek, G., Baglioni, P., Gianfiglio, G., Santovincenzo, A., Bayon, S. & van Winnendael, M. (2006). ExoMars: searching for Life on the Red Planet. *ESA Bull.* **126**, 17–23.

Warren, S.G. (1984). Optical constants of ice from the ultraviolet to the microwave. *Appl. Opt.* **23**(8), 1206–1225.

Weinstein, S. *et al.* (2008). Application of pulsed-excitation fluorescence imager for daylight detection of sparse life in tests in the Atacama Desert. *J. Geophys. Res.* **113**(G1), G01S90.

Wynn-Williams, D.D. & Edwards, H.G.M. (2000). Antarctic ecosystems as models for extraterrestrial surface habitats. *Planet. Space Sci.* **48**, 1065–1075.

Ziegmann, M., Abert, M., Müller, M. & Frimmel, F.H. (2010). Use of fluorescence fingerprints for the estimation of bloom formation and toxin production of Microcystis aeruginosa. *Water Res.* **48**, 195–204.

https://doi.org/10.1017/S1473550413000335 Published online by Cambridge University Press